MACEIÓ - ALAGOAS
EBA 15
15° ENCONTRO BRASILEIRO SOBRE ADSORÇÃO
15th Brazilian Meeting about Adsorption

Synthesis and characterization of NiFe/LDH_CQD composite materials for adsorption applications

Larissa F. Queiroz[a,*], Danilo H. S. Santos[a], Luiz D. da Silva Neto[b], Johnnatan D. de Freitas[c], Lucas Meili[a]

[a] *Technology Center of Federal University of Alagoas, Av. Lourival Melo Mota, s/n, Maceió-AL, 57072-970, Brazil*
[b] *Polytechnic School, Federal University of Bahia, Rua Professor Aristides Novis 02, Salvador-BA, 40210-630, Brazil*
[c] *Chemistry Coordinator of Federal Institute of Alagoas, Av. Railway No. 530, Center, Maceió-AL, 57020-600, Brazil*

Abstract

In this work, a composite material of Carbon Quantum Dots (CQDs) obtained from cashew leaves (Anacardium occidentale L.) supported on NiFe/Layered Double Hydroxide for application as an adsorbent was produced. The materials were synthesized using different routes and characterized by photoluminescence spectroscopy (PL), FTIR, XRD, and SEM. The results show that the composite was successfully produced when the synthesis was carried out using the hydrothermal method without nitrogen. This result contributes significantly to the production of high-quality adsorbents.

Keywords: composite materials; carbon quantum dot; layered double hydroxide; synthesis; characterization;

1. Introduction

Significant efforts have been made to find solutions to the water pollution problem; however, it remains a considerable challenge. In this context, Layered Double Hydroxides (LDHs) stand out as versatile materials due to their two-dimensional sheet-like structure, which endows them with various properties suitable for applications such as adsorption and catalysis [1, 2, 3]. Another noteworthy material for such applications is CQD, which belongs to the carbon family and exhibits properties such as low toxicity, photo-stability, biocompatibility, and high surface area, among others [4]. Consequently, CQDs can provide anchoring sites and active sites that facilitate the synthesis of multicomponent composite materials [5]. This study aims to synthesize and characterize CQD-supported NiFe/LDH composites and evaluate their efficiency as adsorbent materials.

2. Materials and Methods

2.1 Carbon Quantum Dot Synthesis

Cashew leaves (Anacardium occidentale L.) were collected while still green, washed with deionized water, and dried in an oven at 60 °C for 24 hours. The dried leaves were then ground to particles smaller than 0.42 mm. Subsequently, 0.5 g of the obtained powder was placed in an autoclave with 20 mL of deionized water, and the reaction was conducted in an oven at 200 °C for 8 hours. Afterward, the autoclave was cooled to room temperature. The reaction solution was filtered to remove impurities from larger particles and then centrifuged at 10,000 rpm for 10 minutes.

2.2 LDH Synthesis by Coprecipitation

Two solutions were prepared for the coprecipitation method. Solution A was an alkaline solution containing 8 g of sodium hydroxide and 1.32 g of sodium carbonate in 100 mL of deionized water, stirred for 30 minutes. Solution B contained 19.194 g of nickel nitrate and 13.332 g of iron nitrate in 20 mL of deionized water, which was stirred until the salts were fully dissolved. Solution A was then slowly added to Solution B while stirring at 1000 rpm for 8 hours, resulting in a brown

paste. This paste was centrifuged and washed several times with deionized water, then dried in an oven at 65 °C for 24 hours.

2.3 LDH/CQD Coprecipitation Synthesis

The only difference in the coprecipitation synthesis of LDH/CQD is the addition of 20 mL of carbon quantum dot solution to Solution A.

2.4 Hydrothermal Synthesis of LDH

Two solutions were prepared similarly to the coprecipitation method in the hydrothermal method. Solution A contained 8 g of sodium hydroxide and 1.32 g of sodium carbonate in 100 mL of deionized water, stirred for 30 minutes. Solution B contained 19.194 g of nickel nitrate and 13.332 g of iron nitrate in 20 mL of deionized water, stirred until fully dissolved. Solution A was added slowly to Solution B with vigorous stirring at 1000 rpm for 1 hour, producing a brown paste. This paste was placed in an autoclave, and the reaction was conducted in an oven at 160 °C for 8 hours. Afterward, it was cooled to room temperature, centrifuged, washed several times with deionized water, and dried in an oven at 65 °C for 24 hours.

2.5 Hydrothermal Synthesis of LDH/CQD

The only difference in the hydrothermal synthesis of LDH/CQD is the addition of 20 mL of carbon quantum dot solution to Solution A.

2.6 Nitrogen-Doped LDH/CQD Synthesis

20 mL of CQD solution was combined with 19.194 g of nickel nitrate, 8.888 g of iron nitrate, 24.028 g of urea, and 3.708 g of ammonium fluoride (NH4F) in 50 mL of deionized water, which was stirred for 30 minutes. The solution was then transferred to a 100 mL Teflon-coated autoclave for a hydrothermal process at 120 °C for 24 hours. After cooling to room temperature, the mixture was centrifuged, washed several times with deionized water, and dried in an oven at 65 °C for 24 hours.

2.7 Characterization of Materials

CQDs were analyzed using fluorescence spectroscopy with a Fluorolog fluorometer (HORIBA), equipped with an FL-1039/40 monochromator, a 450 W xenon lamp, and an R928P photomultiplier detector. To verify the presence of CQDs in the CQD-supported NiFe/LDH composites, 0.5 g of each material was added to 10 mL of solutions with pH 3 and pH 4, stirred for 2 hours, and analyzed by photoluminescence spectroscopy. X-ray diffraction was performed using a Shimadzu XRD-6000 diffractometer equipped with a Ni filter and a CuKα radiation source (λ = 0.1542 nm), with a voltage of 30 kV and a current of 30 mA. Data were recorded in the 2θ range from 5° to 80°. FTIR-ATR analyses were conducted using a Shimadzu FTIR PRESTIGE 21 spectrophotometer in the spectral range of 4000 cm^{-1} to 400 cm^{-1}. The samples were examined under a scanning electron microscope (Tescan VEGA-3 LMU, Brno, Kohoutovice, Czech Republic).

3. Results

3.1 Photoluminescence Spectroscopy

The emission spectra with varying excitation of the CQD were investigated in the range of 280–420 nm (Fig. 1A). The results show that with an increase in λex, the emission band increased until it was centered at 300 nm and then started to decrease. Additionally, it was observed that the emission depends on the excitation, with a shift towards the red region.

The photoluminescence spectroscopy analysis of the produced materials (Fig. 1B), with an excitation band of 300 nm, revealed the presence of CQD in the NiFe/LDH_CQD_HT material, which is a carbon quantum dot supported on LHD formed via hydrothermal synthesis.

3.2 Fourier Transform Infrared Spectroscopy (FTIR)

The FTIR spectra of the NiFe/LDH samples (Tab. 1) show a double peak in the 3700–3600 cm^{-1} range, related to the O–H stretching vibrations of structural hydroxyl groups and adsorbed water. In addition, there is a prominent peak in the 2366–2300 cm^{-1} range, leaving the stretching and angular deformation of the C–C bond. The range of 1600–1500 cm^{-1} corresponds to the C=C bond, which may indicate the presence of CQD on the surface of NiFe/LDH. This interaction facilitates the conjugation of the π electrons present on the carbon

surface with the electrons of the aromatic e of the organic dye, resulting in the formation of a conjugated π–π electron system [6, 7, 8].

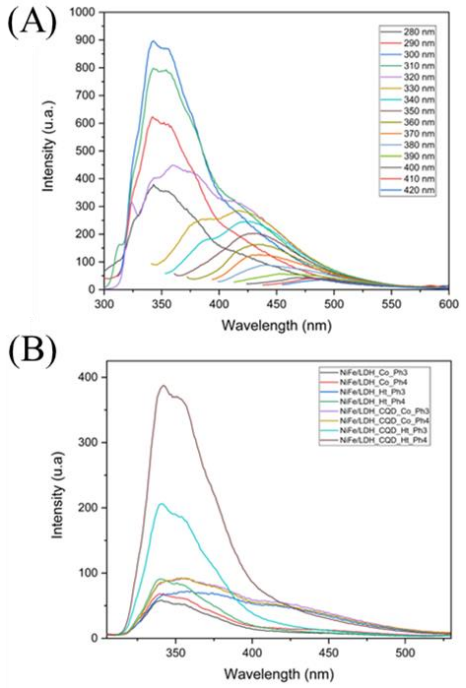

Fig. 1. Images of photoluminescence spectroscopy. A) Emission spectra with varied excitation of the CQD; B) Analysis of the presence of CQDs in the produced materials.

Table 1. FTIR spectra of the synthesized materials. (A) NiFe/LDH by coprecipitation; (B) NiFe/LDH hydrothermal; (C) NiFe/LDH_CQD by coprecipitation; (D) NiFe/LDH_CQD hydrothermal; (E) NiFe/LDH_CQD_N.

	Sample				
Wavenumber (cm^{-1})	**A**	**B**	**C**	**D**	**E**
3740	✓	✓	✓	✓	✓
3630	✓	-	✓	✓	✓
2360	✓	✓	✓	✓	✓
2330	✓	✓	✓	✓	✓
1600	✓	✓	-	✓	✓
1511	✓	✓	✓	✓	✓
677	✓	✓	✓	✓	✓
450	✓	✓	-	✓	✓

The band located in the range of 1400–1300 cm-1 for NiFe/LDH corresponds to the C─O bonds of CO3-2 present in the LDH interlayer. Note that this peak is smooth in carbon quantum dot-containing materials and residues in nitrogen-doped quantum dot materials. The 750–500 cm-1 bands may represent metal-oxygen (M–O) stretching vibrations, bringing Fe–O and Ni–O bond vibrations in NiFe/LDH [7, 8]. The results indicate that the materials present the same characteristic peaks even after doping.

3.3 X-Ray Diffraction (XRD)

X-ray diffraction analysis revealed (Tab. 2) that all materials exhibit intense peaks at 2θ values of (003), (006), (015), (018), (110), and (113). These peaks are characteristic of NiFe/LDH (JCPDS No. 49-188) [7].

Moreover, the intense, sharp, and symmetric peaks at lower 2θ values and weak, less pronounced, and asymmetric peaks at higher 2θ values suggest that the materials exhibit a well-ordered layered structure [8].

The NiFe/LDH_CQD_N sample presented sharper and more intense peaks, implying better crystallinity of this material. Additionally, the NiFe/LDH exhibited additional peaks at 2θ values of 30.09°, 36.02°, 43.79°, 57.63°, and 63.22°. These peaks correspond to the basal planes of (111), (220), (311), (400), (511), and (440), respectively, which are characteristic peaks of magnetite (Fe3O4) (JCPDS No. 19-0629). This result indicated the formation of magnetite nanoparticles during the hydrothermal treatment.

Table 2. X-ray diffraction spectra of the synthesized materials. (A) NiFe/LDH by coprecipitation; (B) NiFe/LDH hydrothermal; (C) NiFe/LDH_CQD by coprecipitation; (D) NiFe/LDH_CQD hydrothermal; (E) NiFe/LDH_CQD_N

Basal Spacing	**Sample**				
(2θ)	**A**	**B**	**C**	**D**	**E**
003	11.16	11.34	11.08	11.98	11.62
006	22.8	23	22.9	22.9	23.4
015	39	39.04	39.04	39.04	39.02
018	47.92	48.04	48.06	47.96	46.64
110	59.86	-	59.82	59.9	59.8
113	61.22	61.8	62.7	61.68	61.22

3.4 Scanning Electron Microscopy (SEM)

The morphologies of the materials were investigated using scanning electron microscopy, as shown in Figure 2. Pure NiFe/LDH, synthesized by coprecipitation (Fig. 2A) and hydrothermal

methods (Fig. 2B), exhibited heterogeneous particle sizes. The NiFe/LDH_CQD composite material synthesized by coprecipitation (Fig. 2C) showed smooth and firm particles, while the hydrothermal NiFe/LDH_CQD material (Fig. 2D) displayed heterogeneous particle sizes. The NiFe/LDH_CQD_N composite material (Fig. 2E) exhibited irregular and crystalline particles, consistent with the XRD data.

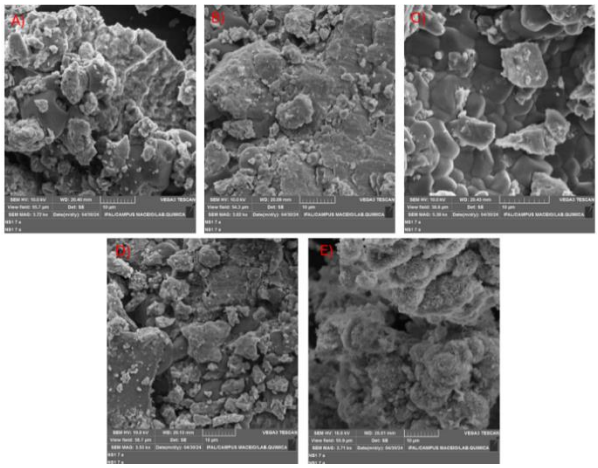

Fig 2. Scanning electron microscopy images of the materials synthesized at 10 kV on a 10 µm scale. A) NiFe/LDH by coprecipitation; NiFe/LDH B) hydrothermal; C) NiFe/LDH_CQD by coprecipitation; D) NiFe/LDH_CQD hydrothermal; E) NiFe/LDH_CQD_N.

4. Conclusion

Based on the results obtained, it was possible to observe that the NiFe/LDH_CQD composite material was efficiently formed when synthesized using the hydrothermal route and without nitrogen doping. Furthermore, the XRD data revealed that all materials exhibited the characteristic peaks of NiFe/LDH, and the FTIR data evidence the possibility of these materials being used as adsorbents due to the functional groups present on their surface.

Acknowledgments

I am grateful to the Federal University of Alagoas, CAPES, FAPEAL, the LAPRO process laboratory, partner laboratories, and my advisor, Lucas Meili.

References

[1] Wang, P., Zhang, X., Zhou, B., Meng, F., Wang, Y., & Wen, G. (2023). Recent advance of layered double hydroxides materials: Structure, properties, synthesis, modification and applications of wastewater treatment. *Journal of Environmental Chemical Engineering*, 111191.

[2] Singh, A., Srivastava, A., Saidulu, D., & Gupta, A. K. (2022). Advancements of sequencing batch reactor for industrial wastewater treatment: Major focus on modifications, critical operational parameters, and future perspectives. *Journal of Environmental Management*, *317*, 115305. [3] Liu, Q., Ma, J., Wang, K., Feng, T., Peng, M., Yao, Z., ... & Komarneni, S. (2017). BiOCl and TiO2 deposited on exfoliated ZnCr-LDH to enhance visible-light photocatalytic decolorization of Rhodamine B. *Ceramics International*, *43*(7), 5751-5758.

[4] Tian, L., Li, Z., Wang, P., Zhai, X., Wang, X., & Li, T. (2021). Carbon quantum dots for advanced electrocatalysis. *Journal of Energy Chemistry*, *55*, 279-294.

[5] Wei, J. S., Ding, C., Zhang, P., Ding, H., Niu, X. Q., Ma, Y. Y., ... & Xiong, H. M. (2019). Robust negative electrode materials derived from carbon dots and porous hydrogels for high-performance hybrid supercapacitors. *Advanced Materials*, *31*(5), 1806197. [3] Roseli Ap. Ferrari*; Vanessa da Silva Oliveira; Ardalla Scabio. Oxidative stability of biodiesel from soybean oil fatty acid ethyl esters. Sci. Agric. (Piracicaba, Braz.), v.62, n.3, p.291-295, May/June 2005.

[4] IATA. Fact Sheet Alternative Fuels. 2016.

[5] Mohammad M, Kandaramath T, Yaakob Z, Chandra Y. Overview on the production of paraffin based-biofuels via catalytic hydrodeoxygenation. Renew Sustain Energy Rev 2013;22:121–32.

[6] Mohammad M, Kandaramath T, Yaakob Z, Chandra Y. Overview on the production of paraffin based-biofuels via catalytic hydrodeoxygenation. Renew Sustain Energy Rev 2013;22:121–32.

[7] Taher, T., Putra, R., Palapa, N. R., & Lesbani, A. (2021). Preparation of magnetite-nanoparticle-decorated NiFe layered double hydroxide and its adsorption performance for congo red dye removal. *Chemical Physics Letters*, *777*, 138712.

[8] Lafi, R., Charradi, K., Djebbi, M. A., Amara, A. B. H., & Hafiane, A. (2016). Adsorption study of Congo red dye from aqueous solution to Mg–Al–layered double hydroxide. *Advanced Powder Technology*, *27*(1), 232-237.